Biol. Chem., Vol. 386, pp. 417–428, May 2005 • Copyright © by Walter de Gruyter • Berlin • New York. DOI 10.1515/BC.2005.050

Evolution of vitamin B_2 biosynthesis: riboflavin synthase of *Arabidopsis thaliana* and its inhibition by riboflavin

Markus Fischer[1,*], Ilka Haase[1], Richard Feicht[1], Nicholas Schramek[1], Peter Köhler[2], Peter Schieberle[2] and Adelbert Bacher[1]

[1] Lehrstuhl für Organische Chemie und Biochemie, Technische Universität München, Lichtenbergstr. 4, D-85747 Garching, Germany

[2] Deutsche Forschungsanstalt für Lebensmittelchemie, Lichtenbergstr. 4, D-85747 Garching, Germany

* Corresponding author
e-mail: markus.fischer@ch.tum.de

Abstract

A synthetic gene specifying the catalytic domain of the *Arabidopsis thaliana* riboflavin synthase was expressed with high efficiency in a recombinant *Escherichia coli* strain. The recombinant pseudomature protein was shown to convert 6,7-dimethyl-8-ribityllumazine into riboflavin at a rate of 0.027 s^{-1} at 25°C. The protein sediments at a rate of 3.9 S. Sedimentation equilibrium analysis afforded a molecular mass of 67.5 kDa, indicating a homotrimeric structure, analogous to the riboflavin synthases of Eubacteria and fungi. The protein binds its product riboflavin with relatively high affinity (K_d=1.1 μM). Product inhibition results in a characteristic sigmoidal velocity versus substrate concentration relationship. Characterization of the enzyme/product complex by circular dichroism and UV absorbance spectroscopy revealed a shift of the absorption maxima of riboflavin from 370 and 445 to 399 and 465 nm, respectively. Complete or partial sequences for riboflavin synthase orthologs were analyzed from 11 plant species. In each case for which the complete plant gene sequence was available, the catalytic domain was preceded by a sequence of 1–72 amino acid residues believed to function as plastid targeting signals. Comparison of all available riboflavin synthase sequences indicates that hypothetical gene duplication conducive to the two-domain architecture occurred very early in evolution.

Keywords: analytical ultracentrifugation; circular dichroism spectroscopy; kinetic analysis; phylogenetic analysis; plant; synthetic gene.

Introduction

Although plants are a major source of vitamin B_2 (Figure 1, riboflavin, **7**) in human and animal nutrition, biosynthesis of the vitamin has been studied predominantly in microorganisms (for review see Young, 1986; Bacher et al., 1996, 2000, 2001). The first committed step catalyzed by GTP cyclohydrolase II involves the hydrolytic release of formate and pyrophosphate from GTP (**3**) (Figure 1). The resulting 2,5-diamino-6-ribosylamino-4(3*H*)-pyrimidinone 5′-phosphate (**4**) is converted into 5-amino-6-ribitylamino-2,4(1*H*,3*H*)-pyrimidinedione (**5**) by the consecutive action of a reductase, a deaminase and a hitherto unidentified phosphatase (Burrows and Brown, 1978; Hollander and Brown, 1979; Nielsen and Bacher, 1981; Richter et al., 1997; Fischer et al., 2004a). Condensation of the pyrimidine derivative **5** with 3,4-dihydroxy-2-butanone-4-phosphate (compound **2**) obtained biosynthetically from ribulose-5-phosphate (**1**) by a complex rearrangement reaction (Volk and Bacher, 1988, 1990) affords 6,7-dimethyl-8-ribityllumazine (**6**) (Kis and Bacher, 1995; Neuberger and Bacher, 1986). Dismutation of that pteridine derivative catalyzed by riboflavin synthase affords riboflavin (**7**) and 5-amino-6-ribitylamino-2,4(1*H*,3*H*)-pyrimidinedione (**5**); the pyrimidine-type side product is subsequently recycled by 6,7-dimethyl-8-ribityllumazine synthase (Maley and Plaut, 1959; Plaut, 1963; Wacker et al., 1964; Plaut and Harvey, 1971; Illarionov et al., 2001a,b; Gerhardt et al., 2002).

A bifunctional protein with GTP cyclohydrolase II and 3,4-dihydroxy-2-butanone 4-phosphate synthase activity from tomato has been cloned and expressed in *E. coli* (Herz et al., 2000). 6,7-Dimethyl-8-ribityllumazine synthase from spinach has been cloned and expressed, and its structure has been determined by X-ray crystallography (Jordan et al., 1999; Persson et al., 1999). Riboflavin synthase has been partially purified from spinach (Mitsuda et al., 1970). The cognate gene has been cloned from *A. thaliana*, but was poorly expressed in *E. coli* (Bacher and Eberhardt, 2001).

This paper describes the efficient heterologous expression, and the biochemical and optical characterization of a pseudomature *A. thaliana* riboflavin synthase. Structural and functional similarities between riboflavin synthases of eubacterial and plant origin are discussed on the basis of bioinformational data.

Results

Sequence analysis with the subcellular location predictor program TargetP (http://www.cbs.dtu.dk./services/TargetP/) suggested that the gene coding for the riboflavin synthase of *A. thaliana* comprises an N-terminal plastid targeting sequence. This agrees with the earlier finding that several other enzymes of the riboflavin pathway in plants carry typical plastid targeting sequences (Jordan et al., 1999; Herz et al., 2000). The chloroplast presequence was calculated using the ChloroP server (http://www.cbs.dtu.dk/services/ChloroP/) predicting a plastid targeting sequence including the amino acid residues 1–69. On the other hand, sequence comparison with bacterial riboflavin synthases suggested a plastid targeting sequence including the amino acid residues

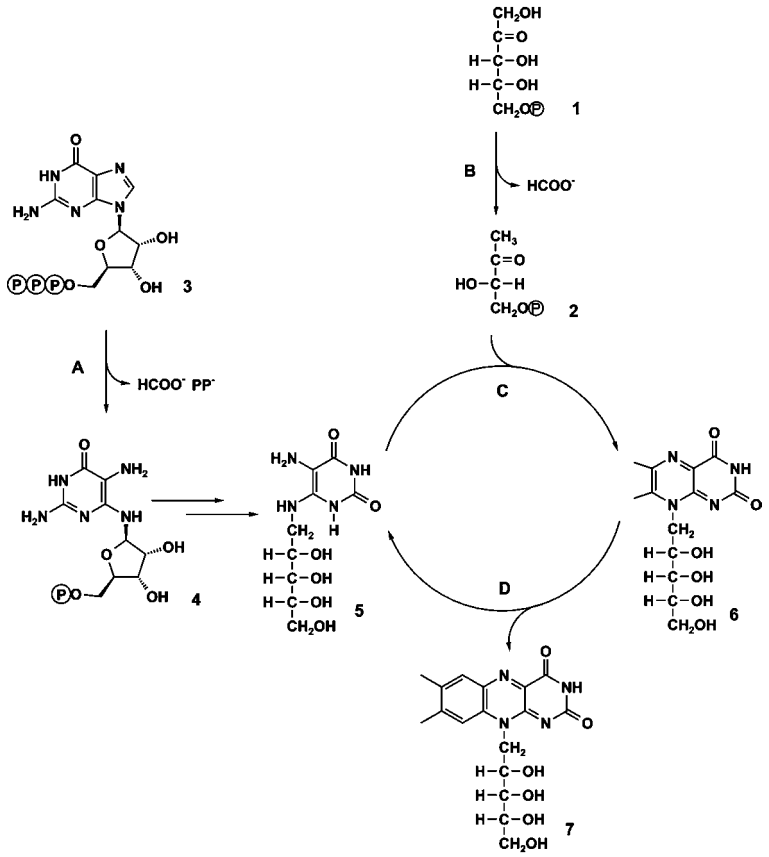

Figure 1 Biosynthesis of riboflavin.
1, ribulose 5-phosphate; **2**, 3,4-dihydroxy-2-butanone 4-phosphate; **3**, GTP; **4**, 2,5-diamino-6-ribosylamino-4(3*H*)-pyrimidinone-5′-phosphate; **5**, 5-amino-6-ribitylamino-2,4(1*H*,3*H*)-pyrimidinedione; **6**, 6,7-dimethyl-8-ribityllumazine; **7**, riboflavin. **A**, GTP cyclohydrolase II; **B**, 3,4-dihydroxy-2-butanone 4-phosphate synthase; **C**, 6,7-dimethyl-8-ribityllumazine synthase; **D**, riboflavin synthase.

1–63. The mature form should thus begin with the N-terminal sequence VFTGIVEE. In this context, it is important to note that the riboflavin synthases of *E. coli* and *Bacillus subtilis* are extremely sensitive to modifications of the N-terminal amino acid segment, although these amino acid residues are not located in the innermost amino acid shell of the ligand-binding site (Illarionov et al., 2001b; Liao et al., 2001; Gerhardt et al., 2002).

The riboflavin synthase gene of *A. thaliana* comprises a substantial number of codons that are poorly translated in *E. coli*, resulting in weak expression (Bacher and Eberhardt, 2001). Therefore, we designed a synthetic gene specifying the amino acid residues 64–271. In the synthetic construct, the codon for valine 64 was replaced by a methionine start codon. The encoded protein closely resembles the *E. coli* enzyme. The synthetic gene was optimized for expression in bacteria by replacement of 59 codons. Moreover, 23 singular restriction sites were introduced to facilitate future sequence modifications (Figure 2). The sequence of the synthetic gene was monitored by DNA sequencing in both directions and has been deposited in the GenBank database (accession number AY604007).

A recombinant *E. coli* strain carrying the synthetic gene under the control of a T5 promoter and *lac* operator produced abundant amounts of a 22-kDa protein (approx. 30% based on total cell protein). The recombinant protein was purified to apparent homogeneity by two chromatographic steps (Figure 3). The purified protein appeared yellow, with absorption maxima at 399 nm and 465 nm (for details see below). Partial Edman degradation afforded the N-terminal sequence MFTGIVEEMG.

A relative mass of 21 171 Da was observed by electrospray mass spectrometry, in excellent agreement with the calculated molecular mass of 21 172 Da.

The enzyme sediments at an apparent velocity of 3.9 S (Svedberg unit) at 20°C. Orthologous riboflavin synthases from various microorganisms have been reported to sediment at similar rates of 3.8–4.4 S (Harvey and Plaut, 1966; Santos et al., 1995; Bacher et al., 1997).

Sedimentation equilibrium experiments indicated a molecular mass of 67.5 kDa using an ideal monodisperse model for calculation. The calculated subunit molecular mass of 22 172 Da implicates a trimer mass of 66.5 kDa, in good agreement with the experimental data (Figure 4).

In order to unequivocally identify the yellow chromophore present in the purified protein solution, aliquots of various batches were treated with trichloroacetic acid, and the supernatant was analyzed by HPLC. The yellow pigment was identified as riboflavin. The non-covalently bound enzyme product could not be removed completely by extensive dialysis. Fluorescence titration experiments afforded a dissociation constant of 1.1 ± 0.04 μM for riboflavin.

To study the optical properties of the riboflavin/enzyme complex, the protein solution was treated with a large

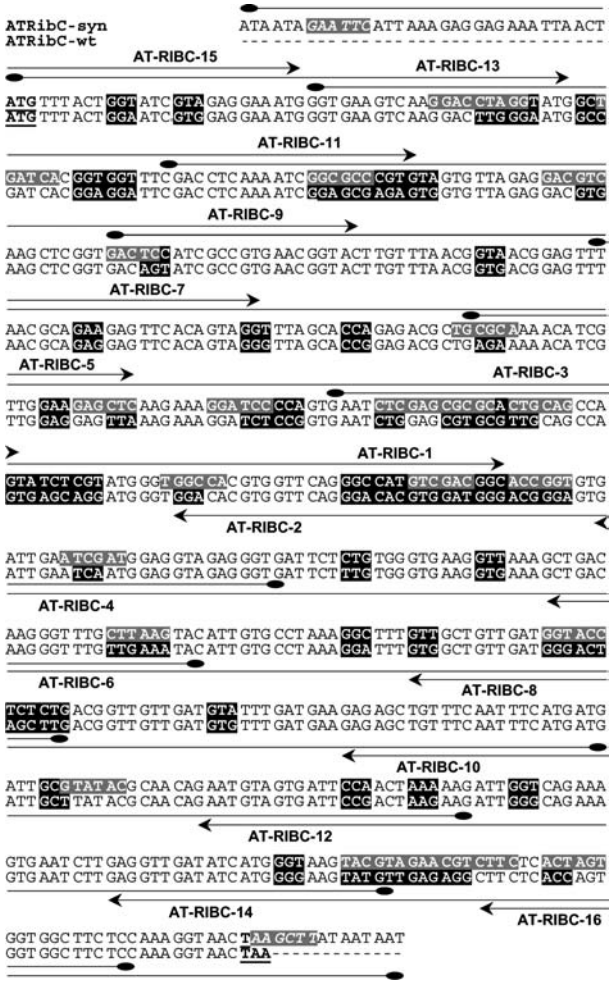

Figure 2 Design of a synthetic gene specifying riboflavin synthase from *A. thaliana.*
Introduced restriction sites are marked in gray and replaced codons are marked in black. Primers refer to Table 2. ATRibC-wt, riboflavin synthase from *A. thaliana* (accession no. AX146690); ATRibC-syn, synthetic gene for the riboflavin synthase from *A. thaliana* (accession no. AY604007).

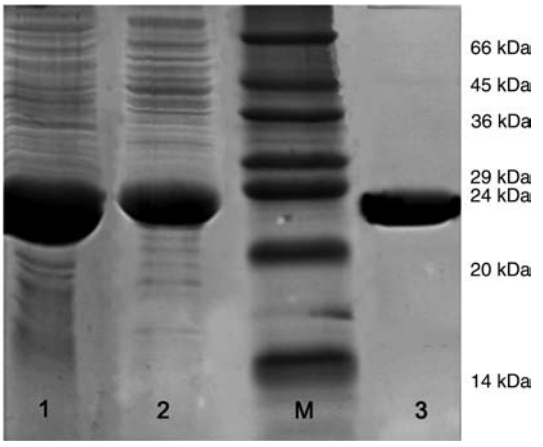

Figure 3 SDS-polyacrylamide gel electrophoresis of riboflavin synthase from *A. thaliana.*
Lane 1, cell extract of *E. coli* M15[pREP4]-pNCO-AT-RibC; lane 2, concentrate after Q-Sepharose chromatography; lane M, molecular mass marker; lane 3, concentrate after Superdex 200 chromatography.

excess of riboflavin and was subsequently dialyzed against 50 mM Tris hydrochloride, pH 7.0. The absorption spectrum of the complex differed from that of free riboflavin in several aspects (Figure 5C). The absorption bands at 370 and 445 nm were shifted to 399 and 465 nm, respectively. The relative intensities of the two bands had changed substantially in comparison with the spectrum of free riboflavin. The circular dichroism (CD) spectrum showed a positive Cotton effect centered at 390 nm and a negative Cotton effect centered at 470 nm (Figure 5B). The CD maxima coincided with those of the absorbance spectrum.

The recombinant, pseudomature plant protein catalyzes the formation of riboflavin from 6,7-dimethyl-8-ribityllumazine at a rate of 0.027 s^{-1} at 25°C and pH 7.3.

Results of steady-state inhibition kinetic experiments are shown in Figure 6. In the initial reaction phase, the velocity curves appear to be sigmoidal, depending on the riboflavin concentration, indicating product inhibition. At high substrate concentrations the reaction velocity decreases, suggesting substrate inhibition. The data could be best approximated using a model according to Scheme 1. The scheme proposes a reaction trajectory taking into account substrate and product inhibition.

With an apparent K_d of 1.1 μM and k_{cat} of 0.027 s^{-1}, inhibition constants can be calculated as 10.9 μM for K_{i2} and 23.7 μM for K_{i3} (Table 1).

The value of the dissociation constant for the binding of the first substrate (K_s) lies in the same range as the dissociation constant for binding of the product (K_d). This is well in line with the fact that the substrate must have the ability to displace riboflavin in the active site to start the reaction. A similar situation exists on comparing the values of the dissociation constant for binding of the second substrate (K_{s2}) and the inhibition constant K_{i2}.

A comprehensive BLAST search using the sequence of the catalytic domain of *A. thaliana* riboflavin synthase as search motif retrieved putative orthologs from higher plants, from blue green algae, from fungi and yeasts, from Eubacteria and two orthologs from Archaebacteria, *Pyrococcus furiosus* and *Halobacterium* NRC-1, respectively. All predicted protein sequences, including the sequences from *P. furious* and *Halobacterium* NRC-1, show the intramolecular sequence similarity that is significant for the subunits of the homotrimeric riboflavin synthases of Eubacteria and fungi, first observed in riboflavin synthase from *B. subtilis* (Schott et al., 1990). More specifically, the hypothetical N- and C-terminal domains of the proteins from *P. furiosu*s and *Halobacterium* NRC-1 share 20.4% and 25.2% identical amino acid residues, respectively.

Three of the putative plant sequences were obviously incomplete (*Marchantia polymorpha*, *Sorghum bicolor*, *Hordeum vulgare*; Figure 7); only a few amino acids of the C-terminal part of the putative sequences of *Lycopersicon esculentum* and *Beta vulgaris* were missing. However, in these two cases the sequence motifs known from the X-ray structure from the ortholog riboflavin synthase of *Schizosaccharomyces pombe* (Gerhardt et al., 2002) believed to participate in the active site are present (Figures 7 and 8). All putative plant sequences believed to represent a full-length riboflavin synthase show the

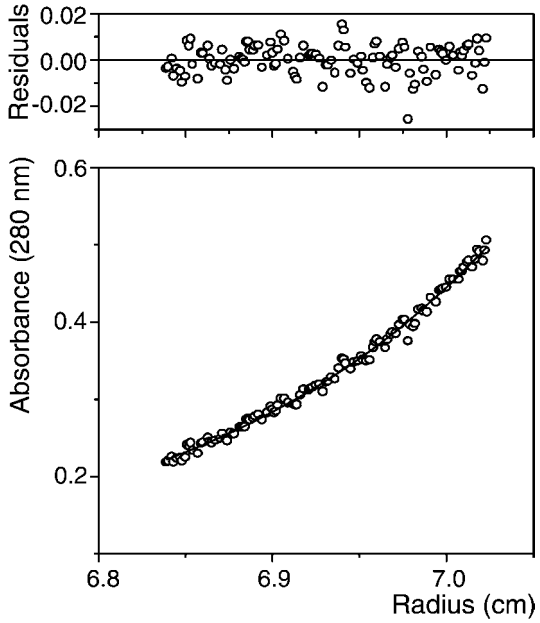

Figure 4 Sedimentation equilibrium centrifugation. Protein concentration was monitored photometrically at 280 nm. The partial specific volume was estimated from the amino acid composition, yielding a value of 0.745 ml g^{-1}.

typical two-domain sequence motifs (Figures 7–9). Notably, the N- and C-terminal subdomains of the taxonomic families Poaceae and Solanaceae form subgroups in the phylogenetic tree (Figure 9). No evidence for the occurrence of more than one riboflavin synthase gene in *A. thaliana* and *Oryza sativa* was obtained using the program tblastn (http://www.ncbi.nlm.nih.gov/BLAST/Genome/PlantBlast.shtml) against the whole genome sequences.

All plant sequences in this study with a full-length N-terminus were preceded by N-terminal segments of up to 72 amino acids in length, which fulfils the criteria for plastid targeting sequences according to the program TargetP.

The sequences of the catalytic domains of all plant enzymes in this study are closely similar (Figure 7), whereas the putative plastid targeting sequences are devoid of significant sequence similarity (data not shown). However, Poaceae and Solanaceae also show sequence similarity in the N-terminal putative targeting regions. For example, the N-terminal parts of *L. esculentum* and *Solanum tuberosum* show 91% identity (screening matrix BLOSUM 62) which fits well with the prevailing opinion that tomato and potato are virtually in the same family. The closest similarity of the *A. thaliana* targeting sequence was the N-terminal part of the ortholog from *Lotus japonicus* (26% identity and 18% strong similarity).

The riboflavin synthases of four plant species (*Triticum aestivum*, *H. vulgare*, *O. sativa* and *S. bicolor*) have glycine-rich insertions in the N-terminal catalytic domain; these are all members of the Poaceae family (Figure 7). Structure-based comparison of these sequences with the available X-ray structures for *E. coli* and *S. pombe* suggested the location of this insertion in the loop connecting β1 and β2 of the N-terminal β barrel (Gerhardt et al., 2002).

The plant sequences show close similarity with riboflavin synthases from yeasts (Figure 10). On the other hand, the similarity of plant riboflavin synthases with those of Cyanobacteria was unexpectedly low.

Not surprisingly, the riboflavin synthases of numerous Gram-negative and -positive bacteria form clusters of similarity. Despite its taxonomic position among the Gram-negative bacteria, *Fusobacterium nucleatum* clusters within the Gram-positive bacteria, which is well in line with the findings of Kapatral et al. (2002) that several features of its core metabolism are similar to that of Gram-positive *Clostridium* spp., *Enterococcus* spp., and *Lactococcus* spp.

Interestingly, the riboflavin synthases of the Archaea *Halobacterium* sp. and *P. furiosus* are similar to those of Eubacteria, fungi and plants, whereas the other completely sequenced Archaebacteria have no riboflavin synthase with similarity to the enzymes under study (Figure 10). Furthermore, the riboflavin synthase of the hyperthermophilic archaeon *P. furiosus* shows a high degree of similarity (53% identity) with the hyperthermophilic eubacterium *Thermotoga maritima.* This result is well in line with the finding that *T. maritima* has a high percentage (24%) of genes that are most similar to archaeal genes (Nelson et al., 1999).

A comprehensive comparison between the N- and C-terminal domains of 73 prokaryotic and eukaryotic riboflavin synthases afforded a highly characteristic dendrogram with two non-overlapping branches (data not shown).

Discussion

The coenzymes derived from riboflavin (vitamin B_2) are characterized by extraordinary chemical versatility. They can catalyze redox processes involving one- and two-electron transitions, as well as a variety of non-redox reactions, such as photorepair of thymidine dimers in photodamaged DNA and the dehydration of non-activated organic substrates (Li and Sancar, 1991; Imada et al., 2003). More recently, they have also been shown to act as chromophores in blue light photoreceptors in plants and fungi (Lin et al., 1995; Ahmad and Cashmore, 1997; Huala et al., 1997; Christie et al., 1999; Schmidt and Galland, 1999; Salomon et al., 2001).

E. coli is a commonly used host strain for the expression of heterologous proteins, but has a bias in codon usage (Kane, 1995; Kurland and Gallant, 1996; Zhou et al., 2004). Eukaryotic organisms often use codons that are rarely used in highly expressed genes of *E. coli* (Nakamura et al., 2000). This biased codon usage hampered the expression of the putative wild-type plant gene in *E. coli*. Re-engineering of the putative gene without affecting the encoded amino acid sequence based on the preferred codon usage of *E. coli* helped to solve this problem. Codon optimization dramatically increased the expression level of the eukaryotic gene in *E. coli*.

The riboflavin synthases of Eubacteria and yeasts have been shown to be homotrimers with unusual properties (Meining et al., 1998; Liao et al., 2001; Gerhardt et al., 2002). The characteristic architecture of riboflavin synthases, consisting of two closely similar folding domains

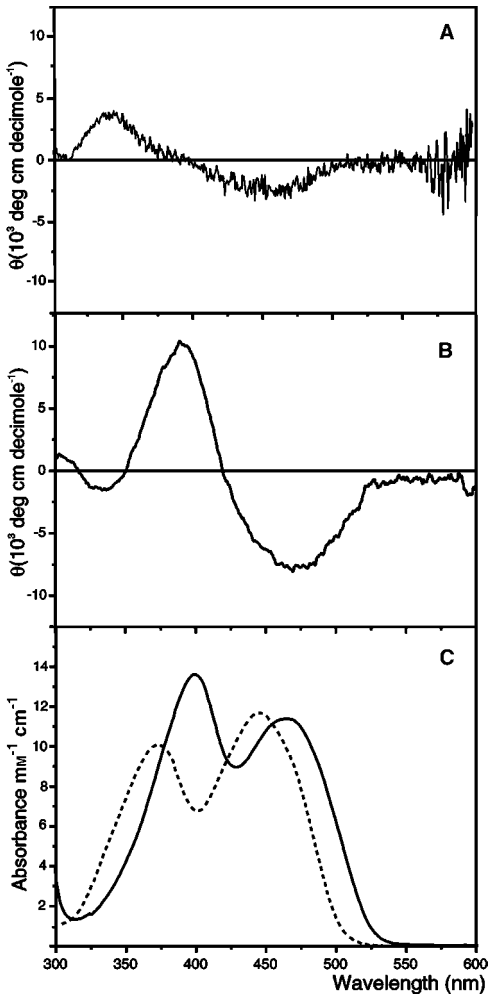

Figure 5 Optical properties of riboflavin in complex with riboflavin synthase from *A. thaliana*.
(A) CD spectrum of riboflavin. (B) CD spectrum of riboflavin bound to riboflavin synthase. (C) Absorption spectra: -----, riboflavin; ——, riboflavin bound to riboflavin synthase. Spectra were obtained in 100 mM Tris hydrochloride, pH 7.

with similar sequences, must be viewed in the context of the unusual reaction mechanism. Briefly, indirect evidence based on X-ray structure analysis of riboflavin synthases from *E. coli* and *S. pombe* suggest that the catalytic reaction proceeds at the interface between the N-terminal domain of one subunit and the C-terminal domain of an adjacent subunit (Liao et al., 2001; Gerhardt et al., 2002). Each of the domains can accommodate one substrate molecule in a shallow surface cavity. The pseudo-c_2-symmetric pairing of two domains involved in catalysis is conducive to the arrangement of the two substrate molecule at the active site in close proximity, with the ribityl side chains pointing into opposite directions. A four-carbon unit is then transferred from the substrate molecule bound at the C-terminal domain to the substrate molecule bound at the N-terminal domain.

Sequence comparison between the proximal and distal domains of the riboflavin synthases from all completely sequenced genomes showed two non-overlapping branches. Hence, gene duplication conducive to the two-domain architecture is believed to have occurred very early in the evolution of riboflavin synthases. Notably, homotrimeric riboflavin synthase molecules can be enclosed in the central cavity of the icosahedral 6,7-dimethyl-8-ribityllumazine synthases of Bacillaceae (Bacher et al., 1980; Ladenstein et al., 1988).

The riboflavin synthases of four Poaceae (*T. aestivum*, *H. vulgare, O. sativa* and *S. bicolor*) have glycine-rich insertions in the N-terminal domain. Structure-based sequence comparison with the ortholog enzyme of *S. pombe* (41% identity, Gerhardt et al., 2002) provides evidence that this insertion is probably located in a surface-exposed loop region.

The riboflavin synthases of plants show close similarity to those of yeasts and Eubacteria. This contrasts in a strange way with the recent finding that the pyrimidine deaminases of the plant riboflavin pathway closely resemble those of Eubacteria, whereas the sequence similarity between plants and yeasts is quite low; more

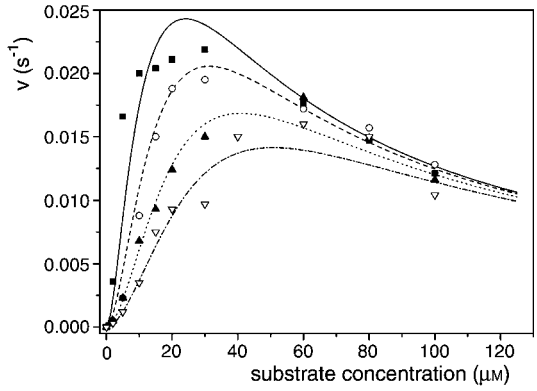

Figure 6 Numerical simulation of inhibition kinetic experiments. Symbols represent experimental data from inhibition experiments. Lines represent numerical simulation using the kinetic constants in Table 1. ■/solid line, 0 μM riboflavin; ○/dotted line, 5.0 μM riboflavin; ▲/dashed line, 15.5 μM riboflavin; ▽/chain dotted line, 31.0 μM riboflavin.

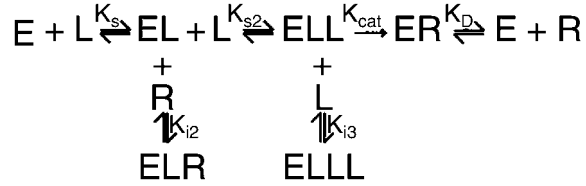

Scheme 1 Reaction scheme used for numerical simulation of the kinetic data.
E, enzyme; L, 6,7-dimethyl-8-ribityllumazine; R, riboflavin.

Table 1 Kinetic constants obtained from inhibition experiments with recombinant riboflavin synthase from *A. thaliana*.

Parameter	Value	Error
k_{cat}	0.027 s^{-1}	(Fixed)
K_d	1.1 μM	(Fixed)
K_s	1.9 μM	1.2 μM
K_{s2}	16.2 μM	2.7 μM
K_{i2}	10.9 μM	4.5 μM
K_{i3}	23.7 μM	1.6 μM

Assays were performed as described under materials and methods.

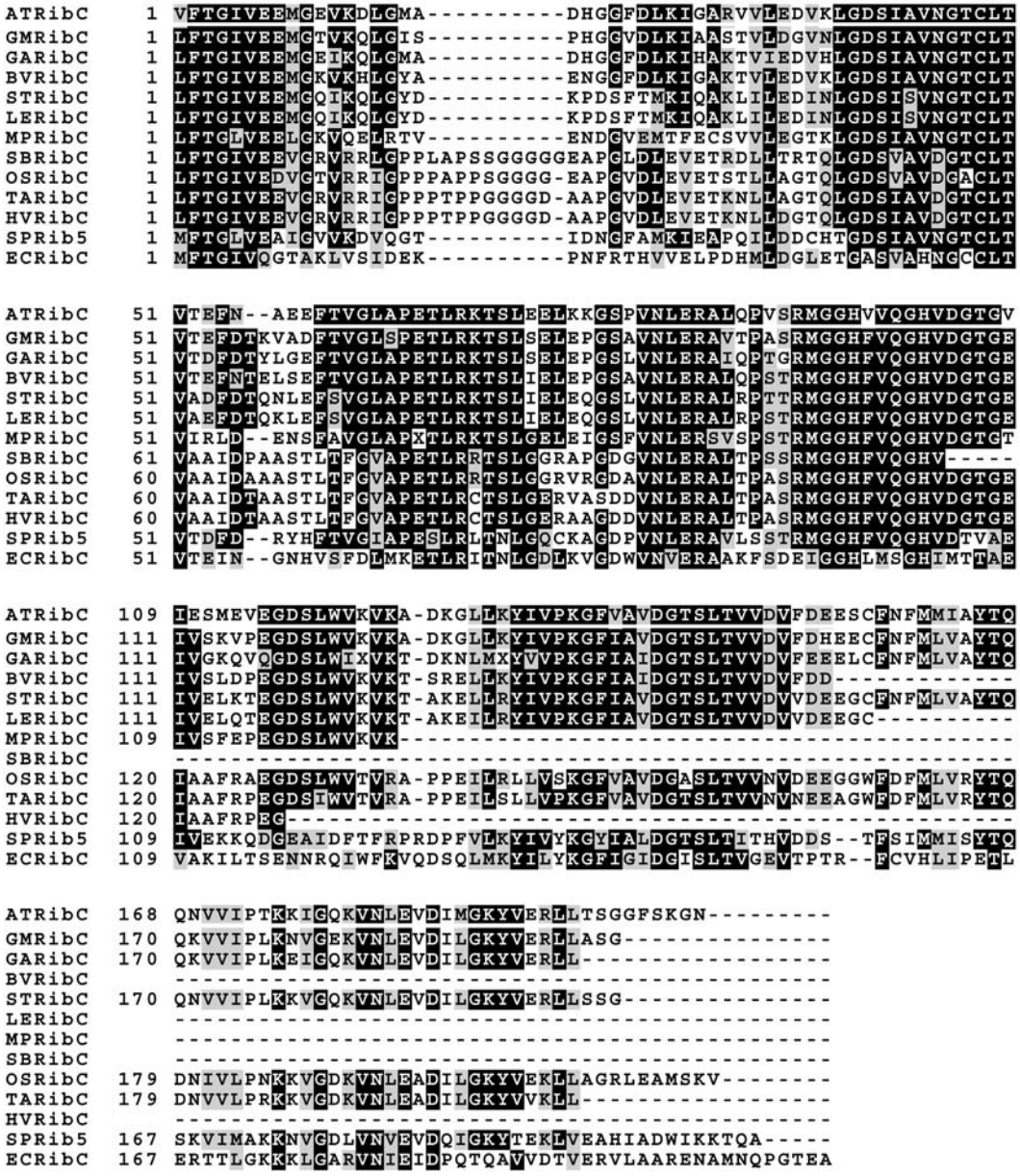

Figure 7 Multiple alignment of riboflavin synthases from different plants, from *S. pombe* and from *E. coli.*
ATRibC, *A. thaliana* (accession no. AX146690); GMRibC, *Glycine max* (accession no. BI787632); GARibC, *G. arboreum* (accession no. BG443237); BVRibC, *B. vulgaris* (accession no. BQ586990); STRibC, *S. tuberosum* (accession no. BQ121327); LERibC, *L. esculentum* (accession no. BI922126); MPRibC, *M. polymorpha* (accession no. AU081711); SBRibC, *S. bicolor* (accession no. CD234043); OSRibC, *O. sativa* (accession no. AL731747); TARibC, *T. aestivum* (accession no. BQ246619); HVRibC, *H. vulgare* (accession no. CB859866); SPRib5, *S. pombe* (accession no. CAB40180); ECRibC, *E. coli* (accession no. P29015). The alignment has been adapted to the catalytic domain of riboflavin synthase. Targeting sequences are not present in the figure. Identical residues are shaded in black; gray boxes indicate those that are chemically similar and may fulfil a comparable function in the proteins.

than that, the yeast and plant deaminases use slightly different substrates (Fischer et al., 2004a).

Riboflavin synthases of the Archaebacteria *Methanococcus jannaschii* and *Methanothermobacter thermoautotrophicus* show no detectable sequence similarity with the homotrimeric riboflavin synthases described in this study. However, they have considerable sequence similarity with 6,7-dimethyl-8-ribityllumazine synthases. Moreover, they share a homopentameric structure with the lumazine synthases (Fischer et al., 2004b).

On the other hand, the genomes of the Archaebacteria *P. furiosus* and *Halobacterium* NRC-1 comprise genes specifying putative proteins with considerable similarity to the riboflavin synthases of Eubacteria, fungi and plants. Notably, the predicted protein sequences from these organisms also show intramolecular sequence similarity that is characteristic of the subunits of the homotrimeric riboflavin synthases of Eubacteria and fungi. Moreover, the riboflavin synthase of *P. furiosus* shows a high degree of similarity with the hyperthermophilic eubacterium *T. maritima*. Completion of the *T. maritima* genome (Nelson et al., 1999) has revealed a degree of similarity with the Archaea in terms of gene content and overall genome organization that was not previously appreciated. Conservation of gene order between *T. maritima* and the Archaea in many of the clustered

Figure 8 Intramolecular sequence similarity of riboflavin synthase subdomains from *A. thaliana* (ATRibC) (without targeting sequence), *E. coli* (ECRibC) and *S. pombe* (SPRib5).
N, N-terminal domain; C, C-terminal domain. Identical residues are shaded in black; similar residues are highlighted in gray. Residues that are believed to interact with the substrate (Gerhardt et al., 2002) are marked by an asterisk.

regions suggests that lateral gene transfer may have occurred between thermophilic Eubacteria and Archaea (Nelson et al., 1999). Nonetheless, the genome of *Halobacterium* NRC-1, which is believed to belong to the Archaea family and which comprises a gene encoding a trimeric eubacterial/yeast/plant-type riboflavin synthase, also contains archaeal type enzymes involved in the early steps of the riboflavin pathway. For instance, no GTP cyclohydrolase II gene, which catalyzes the first step of the biosynthesis in Eubacteria, yeast and plants, is found in the genome of *Halobacterium* NRC-1, but rather a GTP cyclohydrolase III, which is believed to occur only in Archaea (Graham et al., 2002).

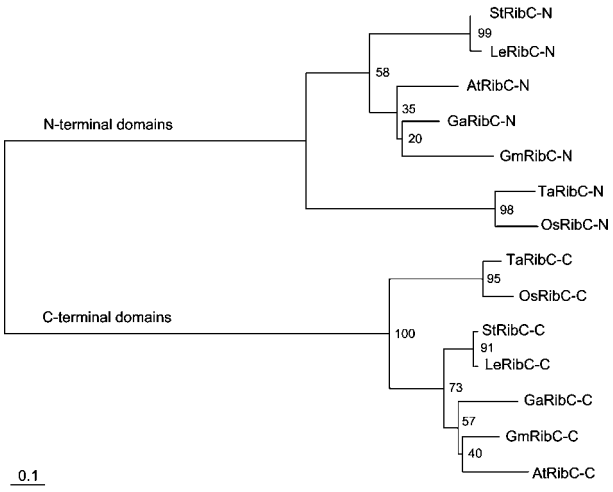

Figure 9 Phylogenetic tree of catalytic subdomains of riboflavin synthases from different plants.
The tree was deduced by neighbor-joining analysis based on the alignment of 14 riboflavin synthase domains. Gaps were removed from the alignment and the total number of positions taken into account was 89. The numbers at the nodes are the statistical confidence estimates computed by the bootstrap procedure. The bar represents distance of 0.1 PAM. The upper cluster represents the N-terminal domain and the lower cluster represents the C-terminal domain. AtRibC, *A. thaliana* (accession no. AX146690); GaRibC, *G. arboreum* (accession no. BG443237); GmRibC, *Glycine max* (accession no. BI787632); StRibC, *S. tuberosum* (accession no. BQ121327); LeRibC, *L. esculentum* (accession no. BI922126); TaRibC, *T. aestivum* (accession no. BQ246619); OsRibC, *O. sativa* (accession no. AL731747).

The purified *A. thaliana* riboflavin synthase was characterized by a bright yellow color. The yellow color was caused by non-covalent binding of riboflavin with a K_d value of 1.1 μM. In contrast, all other riboflavin synthases studied so far were isolated without bound riboflavin, indicating significantly lower affinity.

Recently, the X-ray structure of the complex of riboflavin synthase from *S. pombe* and 6-carboxyethyl-7-oxo-8-ribityllumazine, a substrate analog inhibitor, was determined (Gerhardt et al., 2002). Structural information for non-ligand-bound wild-type riboflavin synthase from *E. coli* is also available (Liao et al., 2001). In addition, the crystal structure of the N-terminal domain of the riboflavin synthase from *E. coli* (Figure 8) in complex with riboflavin has been investigated at high resolution (Meining et al., 2003). However, it should be noted that the naturally occurring *E. coli* riboflavin synthase has very low affinity for its product riboflavin. The conformation of the active-site residues of the domain complex closely resembled the conformation of homologous residues in the native enzymes from *E. coli* and *S. pombe*. Structural superposition with the complex structure of *S. pombe* showed that the orientation and position of the bound ligand and the riboflavin in the domain structure are almost identical (Meining et al., 2003). Comparison of the riboflavin synthase from *A. thaliana* with the primary structures of the enzymes from *E. coli* and *S. pombe* shows that all residues believed to interact with the substrate or the product riboflavin are highly conserved and present in the plant enzyme, suggesting a similar ligand-binding mode (Figure 8).

In addition, ligand-binding studies with *A. thaliana* riboflavin synthase showed that riboflavin is bound in a 1:1 ratio; i.e., one subunit can bind one molecule of riboflavin. These results are well in line with earlier ligand-binding and modeling studies (Otto and Bacher, 1981; Meining et al., 2003).

Furthermore, the absorbance and CD spectra of riboflavin bound to the plant enzyme (Figure 5) are identical to the spectra obtained using the artificial domain of *E. coli* riboflavin synthase (Eberhardt et al., 2001). Tentatively, the long-wavelength transition can be interpreted as a charge transfer complex between the ligand and the protein. However, no stacking interaction between the isoalloxazine ring and an aromatic residue is observed, either

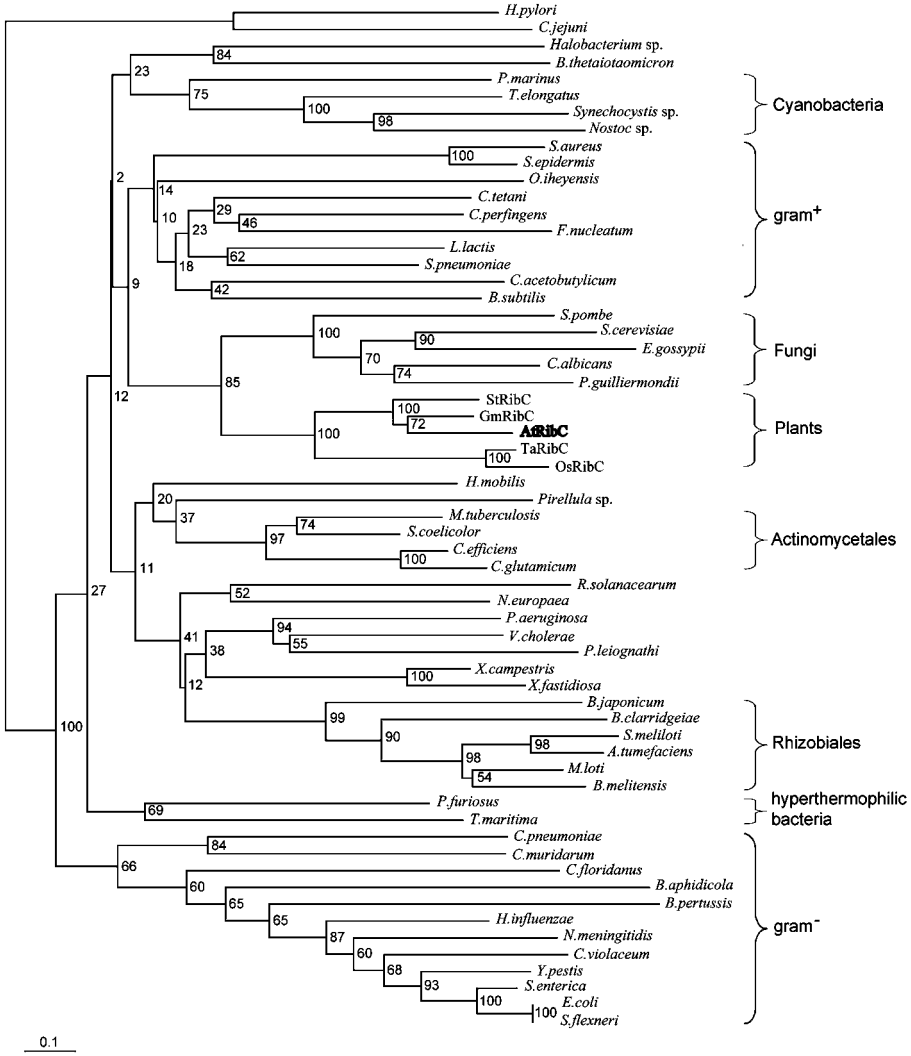

Figure 10 Phylogenetic tree of riboflavin synthases from different organisms.
The tree was deduced by neighbor-joining analysis based on the alignment of 61 riboflavin synthases. Gaps were removed from the alignment and the total number of positions taken into account was 180. The numbers at the nodes are the statistical confidence estimates computed by the bootstrap procedure. The bar represents distance of 0.1 PAM. *Agrobacterium tumefaciens* (strain C58, Dupont) (accession no. AG2720), *A. thaliana* (accession no. AX146690), *Bacillus subtilis* (accession no. A35711), *Bacteroides thetaiotaomicron* VPI-5482 (accession no. NP_810230), *Bartonella clarridgeiae* (accession no. CAB63088), *Bordetella pertussis* (accession no. CAE43146), *Buchnera aphidicola (Baizongia pistaciae)* (accession no. NP_777736), *Bradyrhizobium japonicum* USDA 110 (accession no. BAC50295), *Brucella melitensis* (accession no. NP_540105), *Campylobacter jejuni* (accession no. NP_282365), *Candida albicans* (accession no. CA4790), *Candidatus* Blochmannia floridanus (accession no. NP_878657), *Chlamydia muridarum* (strain Nigg) (accession no. G81675), *Chlamydophila pneumoniae* TW-183 (accession no. NP_876825), *Chromobacterium violaceum* ATCC 12472 (accession no. AAQ60059), *Clostridium perfringens* (strain 13) (accession no. BAB80273), *Clostridium acetobutylicum* (accession no. NP_347229), *Clostridium tetani* E88 (accession no. NP_781340), *Corynebacterium efficiens* YS-314 (accession no. BAC18525), *Corynebacterium glutamicum* ATCC 13032 (accession no. NP_600810), *Eremothetium gossypii* (accession no. AE016908), *E. coli* (accession no. P29015), *Fusobacterium nucleatum* subsp. *nucleatum* ATCC 25586 (accession no. AAL93633), *Glycine max* (accession no. BI787632), *Haemophilus influenzae* (accession no. E64132), *Halobacterium* sp. NRC-1 (accession no. NP_281179), *Heliobacillus mobilis* (accession no. AAN87464), *Helicobacter pylori* J99 (accession no. AAD07067), *Lactococcus lactis* subsp. *lactis* (strain IL1403) (accession no. B86749), *Mesorhizobium loti* (accession no. BAB54295), *Mycobacterium tuberculosis* H37Rv (accession no. CAB02162), *Neisseria meningitidis* (strain MC58 serogroup B) (accession no. D81106), *Nitrosomonas europaea* ATCC 19718 (accession no. NP_842544), *Nostoc* sp. (strain PCC 7120) (accession no. AB2463), *Oceanobacillus iheyensis* HTE831 (accession no. NP_694137), *O. sativa* (accession no. AL731747), *Photobacterium leiognathi* (accession no. JC1187), *Pichia guilliermondii* (accession no. AF459790), *Pirellula* sp. (accession no. NP_870472), *Prochlorococcus marinus* subsp. *pastoris* str. CCMP1986 (accession no. CAE18901), *Pseudomonas aeruginosa* (strain PAO1) (accession no. G83137), *P. furiosus* DSM 3638 (accession no. NP_577790), *Ralstonia solanacearum* (accession no. CAD14244), *Saccharomyces cerevisiae* (accession no. S34072), *Salmonella enterica* subsp. *enterica* serovar Typhi (accession no. NP_456104), *S. pombe* (accession no. T40995), *Shigella flexneri* 2a str. 2457T (accession no. NP_837349), *Sinorhizobium meliloti* (accession no. CAC45790), *S. tuberosum* (accession no. BQ121327), *Staphylococcus aureus* subsp. *aureus* MW2 (accession no. BAB95575), *Staphylococcus epidermidis* ATCC 12228 (accession no. AAO05039), *Streptococcus pneumoniae* R6 (accession no. NP_357757), *Streptomyces coelicolor* A3(2) (accession no. CAC17561), *Synechocystis* sp. (strain PCC 6803) (accession no. S76049), *Thermosynechococcus elongatus* BP-1 (accession no. BAC09238), *T. maritima* (accession no. NP_229624), *T. aestivum* (accession no. BQ246619), *Vibrio cholerae* (strain N16961 serogroup O1) (accession no. E82098), *Xanthomonas campestris* pv. *campestris* str. ATCC 33913 (accession no. NP_636087), *Xylella fastidiosa* Temecula (accession no. AAO29581), *Yersinia pestis* CO92 (accession no. CAC91186). **F. nucleatum* belongs to the Gram-negative bacteria; however, several features of its metabolism are similar to that of some Gram-positive bacteria. ***Halobacterium* sp. NRC-1 and *P. furiosus* belong to the superkingdom of Archaea.

Table 2 Oligonucleotides used for the construction of expression plasmids.

Designation	Sequence (5′ to 3′)
AT-RibC-1	GAATCTGGAGCGCGCACTGCAGCCAGTATCTCGTATGGGTGGCCACGTGGTTCAGGGCCATGTCGACGGC
AT-RibC-2	CACCCTCTACCTCCATCGATTCAATCACACCGGTGCCGTCGACATGGCCCTGAACCACGTGGCC
AT-RibC-3	GCGCAAAACATCGTTGGAAGAGCTCAAGAAAGGATCCCCAGTGAATCTGGAGCGCGCACTGCAGCCAG
AT-RibC-4	GTACTTAAGCAAACCCTTGTCAGCTTTAACCTTCACCCACAGAGAATCACCCTCTACCTCCATCGATTCAATC
AT-RibC-5	TTAACGCAGAAGAGTTCACAGTAGGTTTAGCACCAGAGACGCTGCGCAAAACATCGTTGGAAGAGCTC
AT-RibC-6	CAGAGAGGTACCATCAACAGCAACAAAGCCTTTAGGCACAATGTACTTAAGCAAACCCTTGTCAGC
AT-RibC-7	GACTCCATCGCCGTGAACGGTACTTGTTTAACGGTAACGGAGTTTAACGCAGAAGAGTTCACAGTAGG
AT-RibC-8	CATCATGAAATTGAAACAGCTCTCTTCATCAAATACATCAACAACCGTCAGAGAGGTACCATCAACAGCAAC
AT-RibC-9	CGACCTCAAAATCGGCGCCCGTGTAGTGTTAGAGGACGTCAAGCTCGGTGACTCCATCGCCGTGAACGGTAC
AT-RibC-10	CTTTTTAGTTGGAATCACTACATTCTGTTGCGTATACGCAATCATCATGAAATTGAAACAGCTCTC
AT-RibC-11	GGGTGAAGTCAAGGACCTAGGTATGGCTGATCACGGTGGTTTCGACCTCAAAATCGGCGCCCGTG
AT-RibC-12	ACGTACTTACCCATGATATCAACCTCAAGATTCACTTTCTGACCAATCTTTTTAGTTGGAATCACTACATTC
AT-RibC-13	ATGTTTACTGGTATCGTAGAGGAAATGGGTGAAGTCAAGGACCTAGGTATG
AT-RibC-14	GGAGAAGCCACCACTAGTGAGAAGACGTTCTACGTACTTACCCATGATATCAACCTC
AT-RibC-15	ATAATAGAATTCATTAAAGAGGAGAAATTAACTATGTTTACTGGTATCGTAGAGGAAATG
AT-RibC-16	TATTATTATAAGCTTAGTTACCTTTGGAGAAGCCACCACTAGTGAGAAG

in the domain structure or in the structure of the yeast enzyme (Gerhardt et al., 2002; Meining et al., 2003). On the other hand it should be noted that replacement of the absolutely conserved phenylalanine 2 by alanine in the *E. coli* riboflavin synthase afforded a completely inactive protein (Illarionov et al., 2001b). Although this mutant could still bind two lumazine-type molecules, the chemical shifts for the ligand bound at the putative N-terminal-binding site, as observed by NMR spectroscopy, were significantly modulated. These findings suggest that the N-terminus of the polypeptide forms an essential part of the active site (Illarionov et al., 2001b). In light of the fact that the riboflavin synthase of *A. thaliana* is highly homologous to eubacterial and yeast orthologs, it cannot be excluded that this phenylalanine residue interacts in some manner with the ligand, resulting in the observed change in optical properties.

Steady-state inhibition kinetic analysis showed significant deviation from Michaelis-Menten behavior. Kinetic data could only be explained using a mixed substrate and product inhibition model. We tentatively suggest that binding of the third substrate proceeds in one of the remaining active sites of the trimeric riboflavin synthase, possibly inducing a conformational change. Substrate inhibition only occurs at non-physiological high lumazine concentrations with a weak inhibition constant of 23.7 μM (Table 1) and can therefore be neglected. Product inhibition, on the other hand, results in a characteristic sigmoidal velocity versus substrate concentration relationship. This behavior is similar to allosteric enzymes. However, it is unclear at the moment whether this product inhibition is used as a feedback regulation mechanism of riboflavin biosynthesis in plants.

Materials and methods

Gene synthesis

The partially complementary oligonucleotides AT-RibC-1 and AT-RibC-2 were annealed and treated with DNA polymerase (Table 2).

The resulting 103-bp segment was elongated by a series of seven PCR amplifications using pairwise combinations of oligonucleotides according to Table 2, the first cycle being performed with the oligonucleotides AT-RibC-3 and AT-RibC-4 (Figure 2). The resulting 664-bp DNA fragment was treated with *Eco*RI and *Hind*III and was ligated into the plasmid pNCO113, which had been treated with the same restriction endonucleases. The ligation mixture was transformed into *E. coli* strain XL-1 Blue, affording the recombinant strain XL-1-pNCO-AT-RibC (Table 3).

Transformants were selected on LB agar plates supplemented with ampicillin (170 mg/l). The plasmid was reisolated and transformed into *E. coli* M15[pREP4] cells carrying the pREP4 repressor plasmid for the overexpression of *lac* repressor protein. Kanamycin (20 mg/l) and ampicillin (170 mg/l) were added to secure the maintenance of both plasmids in the host strain. In the pNCO113 expression plasmid, the riboflavin synthase gene is under the control of a T5 promoter and a *lac* operator.

Purification of riboflavin synthase

The recombinant *E. coli* strain M15[pREP4]-pNCO-AT-RibC was grown in LB medium containing ampicillin (170 mg/l) and kanamycin (20 mg/l) at 37°C with shaking. At an optical density of 0.6 (600 nm), isopropylthiogalactoside was added to a final concentration of 2 mM, and incubation was continued at 37°C with shaking. After 5 h, cells were harvested by centrifugation, washed with 0.9% NaCl and stored at -20°C.

Table 3 Bacterial strains and plasmids used in this study.

Strain or plasmid	Relevant characteristics	Source
E. coli strain XL-1-Blue	*recA1*, *endA1*, *gyrA96*, *thi-1*, *hsdR17*, *supE44*, *relA1*, *lac*[*F′*, *proAB*, *lacI*^{q}*ZΔM15*, *Tn10(tet*^{r}*)*]	Bullock et al., 1987
E. coli strain M15[pREP4]	*lac, ara, gal, mtl, recA*$^{+}$*, uvr*$^{+}$*,* [*pREP4: lacI, kan*^{R}]	Zamenhof and Villarejo, 1972
Plasmid pNCO113	Expression vector	Stueber et al., 1990
pNCO-AT-RibC	*RibC* gene of *A. thaliana*	This study

Frozen cell paste (3.5 g) was thawed in 30 ml of 50 mM Tris hydrochloride, pH 7.1 (buffer A). The suspension was cooled on ice, ultrasonically treated and centrifuged. The supernatant was placed on a Q-Sepharose FF column (64 ml) equilibrated with buffer A. The column was developed with a linear gradient of 0–1.0 M potassium chloride in buffer A. Fractions were combined and concentrated by ultrafiltration. The solution was placed on top of a Superdex-200 column (2.6×60 cm) and developed with buffer A containing 100 mM potassium chloride. Fractions were combined and concentrated by ultrafiltration.

Estimation of protein concentration

Protein concentration was estimated by a modified Bradford procedure as reported by Read and Northcote (1981).

SDS polyacrylamide gel electrophoresis

Sodium dodecyl sulfate-polyacrylamide gel electrophoresis was performed with 16% polyacrylamide gels (Laemmli, 1970). Molecular weight standards were supplied by Sigma (Munich, Germany).

DNA sequencing

Sequencing was performed by the Sanger dideoxy chain termination method (Sanger et al., 1977) using a model 377A DNA sequencer from Applied Biosystems (Foster City, CA, USA).

Protein sequencing

Protein solution (50 pmol of protein) was applied to a ProSorb® dot-blotting device, which had been previously activated with 10 μl of methanol. A polyvinylidene fluoride (PVDF) membrane was washed with water (700 μl), air-dried, removed from the device and placed into the cartridge of a Procise 492 protein sequencer (Applied Biosystems, Weiterstadt, Germany). Sequence analysis was then carried out by automated Edman degradation in the pulsed-liquid mode (Edman and Henschen, 1975).

High-performance liquid chromatography

Protein was denatured with 15% (w/v) trichloroacetic acid. The mixture was centrifuged, and the supernatant was analyzed using a column of Hypersil ODS, 5 μm. The eluent contained 100 mμ ammonium formate and 40% (v/v) methanol. The effluent was monitored fluorimetrically (6,7-dimethyl-8-ribityllumazine: excitation, 408 nm; emission, 487 nm; flavins: excitation, 445 nm; emission, 520 nm).

Fluorescence titration

Experiments were performed with a type F-2000 spectrofluorimeter from Hitachi at room temperature in a 10-mm quartz cell as previously described (Fischer et al., 2002).

Steady-state kinetics

Assay mixtures contained 100 mM potassium phosphate, pH 7.3, 10 mM EDTA, 10 mM sodium sulfite and 1.4 μM enzyme (subunits). 6,7-Dimethyl-8-ribityllumazine was added as indicated. The mixtures were incubated at 25°C and were monitored photometrically at 470 nm. The absorbance coefficient for riboflavin at 470 nm is 9100 M^{-1} cm^{-1} (Plaut et al., 1970; Plaut and Harvey, 1971). For inhibition kinetics, different amounts of riboflavin (5.0, 15.5 and 31.0 μM) were added to the assay mixtures. The data sets were analyzed using the program DynaFit version 3.28.024 (Kuzmic, 1996). The absorbance coefficient for enzyme-bound riboflavin at 470 nm was calculated from absorbance spectra, resulting in a value of 9500 M^{-1} cm^{-1}.

Circular dichroism

Measurements were performed with a JASCO J-715 spectropolarimeter as previously described (Fischer et al., 2002).

Electrospray mass spectrometry

Experiments were performed by published procedures (Mann and Wilm, 1995) using a triple quadrupole ion spray mass spectrometer (API365; SciEx, Thornhill, ON, Canada).

Analytical ultracentrifugation

Experiments were performed with an Optima XL-A analytical ultracentrifuge from Beckman Instruments (Palo Alto, CA, USA) equipped with absorbance optics. Aluminum double-sector cells equipped with quartz windows were used throughout. The partial specific volume was estimated from the amino acid composition (Laue et al., 1992). Protein concentration was monitored photometrically at 280 nm.

For boundary sedimentation experiments, a solution containing 50 mM Tris hydrochloride, pH 7.0, 100 mM potassium chloride and 2.3 mg of protein per ml was centrifuged at 59 000 rpm and 20°C.

Sedimentation equilibrium experiments were performed with a solution containing 0.75 mg of protein per ml of 50 mM Tris hydrochloride, pH 7.0, containing 300 mM potassium chloride. Samples were centrifuged at 10 000 rpm and 4°C for 72 h.

Sequence alignment and phylogenetic analysis

Amino acid sequences of *A. thaliana* (accession no. AY604007) riboflavin synthase was used to query non-redundant NCBI (http://www.ncbi.nlm.nih.gov/) and plant cDNA/EST databases (http://www.plantgdb.org/cgi-bin/PlantGDBblast) using the BLAST algorithm (Altschul and Koonin, 1998). Protein sequences were aligned using ClustalW (http://clustalw.genome.ad.jp/). Phylogenetic analyses of the aligned amino acid sequences were performed using the Phylogeny Interference Package PHYLIP 3.57c (Felsenstein, 1995) and PHYLO_WIN (Galtier et al., 1996). Phylogenetic trees were constructed by the neighbor-joining method. The Dayhoff (1979) PAM 001 matrix was used to calculate distances between pairs of protein sequences. A bootstrap analysis using 1000 iterations was performed (Felsenstein, 1985).

Acknowledgments

We thank Sebastian Schwamb and Thomas Wojtulewicz for skillful help in protein preparation. This work was supported by the Deutsche Forschungsgemeinschaft and the Fonds der Chemischen Industrie.

References

Ahmad, M. and Cashmore, A.R. (1997). The blue-light receptor cryptochrome 1 shows functional dependence on phytochrome A or phytochrome B in *Arabidopsis thaliana*. Plant J. *11*, 421–427.

Altschul, S.F. and Koonin, E.V. (1998). Iterated profile searches with PSI-BLAST – a tool for discovery in protein databases. Trends Biochem. Sci. *23*, 444–447.

Bacher, A. and Eberhardt, S. (2001). Cloning and characterization of riboflavin synthase from *Arabidopsis thaliana* and screening for riboflavin synthase-inhibiting herbicides. PCT International Patent Application WO 0134813, 45 pp.

Bacher, A., Schnepple, H., Mailaender, B., Otto, M.K., and Ben-Shaul, Y. (1980). Structure and function of the riboflavin synthase complex of *Bacillus subtilis*. In: Flavins and Flavoproteins, Proceedings of the 6th International Symposium. pp. 579–586.

Bacher, A., Eberhardt, S., and Richter, G. (1996). Biosynthesis of riboflavin. In: *Escherichia coli and Salmonella typhimurium*: Cellular and Molecular Biology, 2nd Ed., Vol. 1. F.C. Neidhardt, J.L. Ingraham, K.B. Low, B. Magasanik, M. Schaechter, and H.E. Umbarger, eds. (Washington, DC, USA: ASM), pp. 657–664.

Bacher, A., Eberhardt, S., Fischer, M., Mörtl, S., Kis, K., Kugelbrey, K., Scheuring, J., and Schott, K. (1997). Biosynthesis of riboflavin: lumazine synthase and riboflavin synthase. Methods Enzymol. *280*, 389–399.

Bacher, A., Eberhardt, S., Fischer, M., Kis, K., and Richter, G. (2000). Biosynthesis of vitamin B_2 (riboflavin). Annu. Rev. Nutr. *20*, 153–167.

Bacher, A., Eberhardt, S., Eisenreich, W., Fischer, M., Herz, S., Illarionov, B., Kis, K., and Richter, G. (2001). Biosynthesis of riboflavin. Vitam. Horm. *61*, 1–49.

Bullock, W.O., Fernandez, J.M., and Short, J.M. (1987). XL-blue: a high efficiency plasmid transforming recA *Escherichia coli* strain with β-galactosidase selection. Biotechniques *5*, 376–379.

Burrows, R.B. and Brown, G.M. (1978). Presence of *Escherichia coli* of a deaminase and a reductase involved in biosynthesis of riboflavin. J. Bacteriol. *136*, 657–667.

Christie, J.M., Salomon, M., Nozue, K., Wada, M., and Briggs, W.R. (1999). LOV (light, oxygen, or voltage) domains of the blue-light photoreceptor phototropin (nph1): binding sites for the chromophore flavin mononucleotide. Proc. Natl. Acad. Sci. USA *96*, 8779–8783.

Dayhoff, M.O. (1979). Atlas of Protein Sequence and Structure, Vol. 5 (Suppl. 3). (Washington, DC, USA: National Biomedical Research Foundation).

Eberhardt, S., Zingler, N., Kemter, K., Richter, G., Cushman, M., and Bacher, A. (2001). Domain structure of riboflavin synthase. Eur. J. Biochem. *268*, 4315–4323.

Edman, P. and Henschen, A. (1975). Sequence determination. In: Protein Sequence Determination (Heidelberg, Germany: Springer Verlag).

Felsenstein, J. (1985). Confidence limits on phylogenies: an approach using the bootstrap. Evolution *39*, 783–791.

Felsenstein, J. (1995). PHYLIP (Phylogeny Interference Package), Version 3.57c. (Distributed by the author). Department of Genetics, University of Washington, Seattle, WA, USA.

Fischer, M., Haase, I., Feicht, R., Richter, G., Gerhardt, S., Changeux, J.P., Huber, R., and Bacher, A. (2002). Biosynthesis of riboflavin: 6,7-dimethyl-8-ribityllumazine synthase of *Schizosaccharomyces pombe*. Eur. J. Biochem. *269*, 519–526.

Fischer, M., Römisch, W., Saller, S., Illarionov, B., Richter, G., Rohdich, F., Eisenreich, W., and Bacher, A. (2004a). Evolution of vitamin B_2 biosynthesis: structural and functional similarity between pyrimidine deaminases of eubacterial and plant origin. J. Biol. Chem. *279*, 36299–36308.

Fischer, M., Schott, A.K., Römisch, W., Ramsperger, A., Augustin, M., Fidler, A., Bacher, A., Richter, G., Huber, R., and Eisenreich, W. (2004b). Evolution of vitamin B_2 biosynthesis. A novel class of riboflavin synthase in Archaea. J. Mol. Biol. *343*, 267–278.

Galtier, N., Gouy, M., and Gautier, C. (1996). SEAVIEW and PHYLO_WIN: Two graphic tools for sequence alignment and molecular phylogeny. Comput. Appl. Biosci. *12*, 543–548.

Gerhardt, S., Schott, A.K., Kairies, N., Cushman, M., Illarionov, B., Eisenreich, W., Bacher, A., Huber, R., Steinbacher, S., and Fischer, M. (2002). Studies on the reaction mechanism of riboflavin synthase: X-ray crystal structure of a complex with 6-carboxyethyl-7-oxo-8-ribityllumazine. Structure *10*, 1371–1381.

Graham, D.E., Xu, H., and White, R.H. (2002). A member of a new class of GTP cyclohydrolases produces formylaminopyrimidine nucleotide monophosphates. Biochemistry *41*, 15074–15084.

Harvey, R.A. and Plaut, G.W. (1966). Riboflavin synthetase from yeast. Properties of complexes of the enzyme with lumazine derivatives and riboflavin. J. Biol. Chem. *241*, 2120–2136.

Herz, S., Eberhardt, S., and Bacher, A. (2000). Biosynthesis of riboflavin in plants. The *ribA* gene of *Arabidopsis thaliana* specifies a bifunctional GTP cyclohydrolase II/3,4-dihydroxy-2-butanone 4-phosphate synthase. Phytochemistry *53*, 723–731.

Hollander, I. and Brown, G.M. (1979). Biosynthesis of riboflavin: reductase and deaminase of *Ashbya gossypii*. Biochem. Biophys. Res. Commun. *89*, 759–763.

Huala, E., Oeller, P.W., Liscum, E., Han, I.S., Larsen, E., and Briggs, W.R. (1997). *Arabidopsis* NPH1: a protein kinase with a putative redox-sensing domain. Science *278*, 2120–2123.

Illarionov, B., Eisenreich, W., and Bacher, A. (2001a). A pentacyclic reaction intermediate of riboflavin synthase. Proc. Natl. Acad. Sci. USA *98*, 7224–7229.

Illarionov, B., Kemter, K., Eberhardt, S., Richter, G., Cushman, M., and Bacher, A. (2001b). Riboflavin synthase of *Escherichia coli*. Effect of single amino acid substitutions on reaction rate and ligand binding properties. J. Biol. Chem. *276*, 11524–11530.

Imada, Y., Iida, H., Ono, S., and Murahashi, S. (2003). Flavin catalyzed oxidations of sulfides and amines with molecular oxygen. J. Am. Chem. Soc. *125*, 2868–2869.

Jordan, D.B., Bacot, K.O., Carlson, T.J., Kessel, M., and Viitanen, P.V. (1999). Plant riboflavin biosynthesis. Cloning, chloroplast localization, expression, purification, and partial characterization of spinach lumazine synthase. J. Biol. Chem. *274*, 22114–22121.

Kane, J.F. (1995). Effects of rare codon clusters on high-level expression of heterologous proteins in *Escherichia coli*. Curr. Opin. Biotechnol. *6*, 494–500.

Kapatral, V., Anderson, I., Ivanova, N., Reznik, G., Los, T., Lykidis, A., Bhattacharyya, A., Bartman, A., Gardner, W., Grechkin, G., et al. (2002). Genome sequence and analysis of the oral bacterium *Fusobacterium nucleatum* strain ATCC 25586. J. Bacteriol. *184*, 2005–2018.

Kis, K. and Bacher, A. (1995). Substrate channeling in the lumazine synthase/riboflavin synthase complex of *Bacillus subtilis*. J. Biol. Chem. *270*, 16788–16795.

Kurland, C. and Gallant, J. (1996). Errors of heterologous protein expression. Curr. Opin. Biotechnol. *7*, 489–493.

Kuzmic, P. (1996). Program DYNAFIT for the analysis of enzyme kinetic data: application to HIV proteinase. Anal. Biochem. *237*, 260–273.

Ladenstein, R., Schneider, M., Huber, R., Bartunik, H.D., Wilson, K., Schott, K., and Bacher, A. (1988). Heavy riboflavin synthase from *Bacillus subtilis*. Crystal structure analysis of the icosahedral beta 60 capsid at 3.3 Å resolution. J. Mol. Biol. *203*, 1045–1070.

Laemmli, U.K. (1970). Cleavage of structural proteins during the assembly of the head of bacteriophage T4. Nature *227*, 680–685.

Laue, T.M., Shah, B.D., Ridgeway, T.M., and Pelletier, S.L. (1992). Computer-aided interpretation of analytical sedimentation data for proteins. In: Analytical Ultracentrifugation in Biochemistry and Polymer Science, S.E. Harding, A.J. Rowe and J.C. Horton, eds. (Cambridge, UK: Royal Society of Chemistry), pp. 90–125.

Li, Y.F. and Sancar, A. (1991). Cloning, sequencing, expression and characterization of DNA photolyase from *Salmonella typhimurium*. Nucleic Acids Res. *19*, 4885–4890.

Liao, D.I., Wawrzak, Z., Calabrese, J.C., Viitanen, P.V., and Jordan, D.B. (2001). Crystal structure of riboflavin synthase. Structure *9*, 399–408.

Lin, C., Robertson, D.E., Ahmad, M., Raibekas, A.A., Jorns, M.S., Dutton, P.L., and Cashmore, A.R. (1995). Association of flavin adenine dinucleotide with the *Arabidopsis* blue light receptor CRY1. Science *269*, 968–970.

Maley, G.F. and Plaut, G.W. (1959). The isolation, synthesis, and metabolic properties of 6,7-dimethyl-8-ribityllumazine. J. Biol. Chem. *243*, 641–647.

Mann, M. and Wilm, M. (1995). Electrospray mass spectrometry for protein characterization. Trends Biochem. Sci. *20*, 219–224.

Meining, W., Tibbelin, G., Ladenstein, R., Eberhardt, S., Fischer, M., and Bacher, A. (1998). Evidence for local 32 symmetry in homotrimeric riboflavin synthase of *Escherichia coli*. J. Struct. Biol. *121*, 53–60.

Meining, W., Eberhardt, S., Bacher, A., and Ladenstein, R. (2003). The structure of the N-terminal domain of riboflavin synthase in complex with riboflavin at 2.6 Å resolution. J. Mol. Biol. *331*, 1053–1063.

Mitsuda, H., Kawai, F., Suzuki, Y., and Yoshimoto, S. (1970). Biogenesis of riboflavin in green leaves. VII. Isolation and characterization of spinach riboflavin synthetase. J. Vitaminol. (Kyoto) *16*, 285–292.

Nakamura, Y., Gojobori, T., and Ikemura, T. (2000). Codon usage tabulated from international DNA sequence databases: status for the year 2000. Nucleic Acids Res. *28*, 292.

Nelson, K.E., Clayton, R.A., Gill, S.R., Gwinn, M.L., Dodson, R.J., Haft, D.H., Hickey, E.K., Peterson, J.D., Nelson, W.C., Ketchum, K.A., et al. (1999). Evidence for lateral gene transfer between Archaea and bacteria from genome sequence of *Thermotoga maritima*. Nature *399*, 323–329.

Neuberger, G. and Bacher, A. (1986). Biosynthesis of riboflavin. Enzymatic formation of 6,7-dimethyl-8-ribityllumazine by heavy riboflavin synthase from *Bacillus subtilis*. Biochem. Biophys. Res. Commun. *139*, 1111–1116.

Nielsen, P. and Bacher, A. (1981). Biosynthesis of riboflavin. Characterization of the product of the deaminase. Biochim. Biophys. Acta *662*, 312–317.

Otto, M.K. and Bacher, A. (1981). Ligand-binding studies on light riboflavin synthase from *Bacillus subtilis*. Eur. J. Biochem. *115*, 511–517.

Persson, K., Schneider, G., Douglas, B.J., Viitanen, P.V., and Sandalova, T. (1999). Crystal structure analysis of a pentameric fungal and icosahedral plant lumazine synthase reveals the structural basis of differences in assembly. Protein Sci. *8*, 2355–2365.

Plaut, G.W. (1963). Studies on the nature of the enzymic conversion of 6,7-dimethyl-8-ribityllumazine to riboflavin. J. Biol. Chem. *238*, 2225–2243.

Plaut, G.W.E. and Harvey, R.A. (1971). The enzymatic synthesis of riboflavin. In: Methods in Enzymology, Volume 18, D.B. McCormick and L.D. Wright, eds. (New York, USA: Academic Press), pp. 515–538.

Plaut, G.W., Beach, R.L., and Aogaichi, T. (1970). Studies on the mechanism of elimination of protons from the methyl groups of 6,7-dimethyl-8-ribityllumazine by riboflavin synthetase. Biochemistry *9*, 771–785.

Read, S.M. and Northcote, D.H. (1981). Minimization of variation in the response to different proteins of the Coomassie blue G dye-biding assay for protein. Anal. Biochem. *116*, 53–64.

Richter, G., Fischer, M., Krieger, C., Eberhardt, S., Lüttgen, H., Gerstenschläger, I., and Bacher, A. (1997). Biosynthesis of riboflavin: characterization of the bifunctional deaminase-reductase of *Escherichia coli* and *Bacillus subtilis*. J. Bacteriol. *179*, 2022–2028.

Salomon, M., Eisenreich, W., Durr, H., Schleicher, E., Knieb, E., Massey, V., Rüdiger, W., Müller, F., Bacher, A., and Richter, G. (2001). An optomechanical transducer in the blue light receptor phototropin from *Avena sativa*. Proc. Natl. Acad. Sci. USA *98*, 12357–12361.

Sanger, F., Niklen, S., and Coulson, A.R. (1977). DNA sequencing with chain-terminating inhibitors. Proc. Natl. Acad. Sci. USA *74*, 5463–5467.

Santos, M.A., Garcia-Ramirez, J.J., and Revuelta, J.L. (1995). Riboflavin biosynthesis in *Saccharomyces cerevisiae*. Cloning, characterization, and expression of the *RIB5* gene encoding riboflavin synthase. J. Biol. Chem. *270*, 437–444.

Schmidt, W. and Galland, P. (1999). Light-induced absorbance changes in *Phycomyces*: evidence for cryptochrome-associated flavosemiquinones. Planta *208*, 274–282.

Schott, K., Kellermann, J., Lottspeich, F., and Bacher, A. (1990). Riboflavin synthases of *Bacillus subtilis*. Purification and amino acid sequence of the α subunit. J. Biol. Chem. *265*, 4204–4209.

Stueber, D., Matile, H., and Garotta, G. (1990). System for high level production in *E. coli* and rapid purification of recombinant proteins: application to epitope mapping, preparation of antibodies and structure function analysis. In: Immunological Methods IV, I. Lefkovits and P. Pernis, eds. (New York, USA: Academic Press), pp. 121–125.

Volk, R. and Bacher, A. (1988). Biosynthesis of riboflavin. The structure of the four-carbon precursor. J. Am. Chem. Soc. *110*, 3651–3653.

Volk, R. and Bacher, A. (1990). Studies on the 4-carbon precursor in the biosynthesis of riboflavin. Purification and properties of L-3,4-dihydroxy-2-butanone-4-phosphate synthase. J. Biol. Chem. *265*, 19479–19485.

Wacker, H., Harvey, R.A., Winestock, C.H., and Plaut, G.W. (1964). 4-(1′-D-Ribitylamino)-5-amino-2,6-dihydroxypyrimidine, the second product of the riboflavin synthetase reaction. J. Biol. Chem. *239*, 3493–3497.

Young, D.W. (1986). The biosynthesis of the vitamins thiamin, riboflavin, and folic acid. Nat. Prod. Rep. *3*, 395–419.

Zamenhof, P. and Villarejo, M. (1972). Construction and properties of *Escherichia coli* strains exhibiting α-complementation of β-galactosidase fragments *in vivo*. J. Bacteriol. *110*, 171–178.

Zhou, Z., Schnake, P., Xiao, L., and Lal, A.A. (2004). Enhanced expression of a recombinant malaria candidate vaccine in *Escherichia coli* by codon optimization. Protein Expr. Purif. *34*, 87–94.

Received December 22, 2004; accepted March 24, 2005